Quantum Cluster Equilibrium Prediction of Liquid Ethanol

Alhadji Malloum[†,◇,*], Zoubeida Dhaouadi[○] and Jeanet Conradie[†,‡]

[†] Department of Chemistry, University of the Free State, PO BOX 339, Bloemfontein 9300, South Africa.

[◇] Department of Physics, Faculty of Science, University of Maroua, PO BOX 46, Maroua, Cameroon.

[○] Laboratoire de Spectroscopie Atomique Moléculaire et Application, Université de Tunis El Manar, Tunis 1060, Tunisie

[‡]Department of Chemistry, UiT - The Arctic University of Norway, N-9037 Tromsø, Norway.

June 20, 2023

ABSTRACT: Quantum cluster equilibrium theory (QCE) has been widely used to determine the properties of pure and binary mixture of liquids. The main limitation of the application of QCE is the exploration of different possible clusters formed by the solvent molecules. Therefore, in this study, we applied the QCE theory to predict liquid properties of ethanol after thorough exploration of the potential energy surfaces (PESs) of the ethanol clusters from dimer to hexamer. The exploration started by generating possible structures using classical molecular dynamics followed by optimizations at the MP2/aug-cc-pVDZ level of theory. 484 different configurations of the ethanol clusters have been finally used in the QCE theory. The results show that the population of liquid ethanol is constituted from the contribution of hexamer, pentamer, and tetramer. In addition, we noted that the ethanol monomer, dimer and trimer do not contribute to the population of liquid ethanol. Furthermore, based on the predicted population of the liquid ethanol, we calculated its infrared spectrum at different temperatures. The calculated infrared spectrum is found to be in qualitative agreement with experiment. Some thermodynamic properties, such as the heat capacity, are also predicted to be in good agreement with experiment.

KEYWORDS: Liquid ethanol, ethanol clusters, quantum cluster equilibrium, liquid thermodynamic properties

1 Introduction

Weinhold has proposed the quantum cluster equilibrium (QCE) theory to describe the equilibrium properties of liquids based on clusters of molecules constituting the liquids [1]. The QCE theory extends the statistical thermodynamics handling of quantum systems. Weinhold has given the detailed implementation of the theory and will be recalled in subsection 2.1. The QCE theory has then been applied initially to understand the liquid properties of water and ammonia [1–3]. Ludwig, Weinhold, and Farrar [2,3] have determined the thermodynamics properties of liquid ammonia as a function of temperature, including the constant-volume specific heat capacity (C_v). Using a simple **ab-initio** quantum mechanical method (HF/6-31+G(d)), the authors have predicted properties with an acceptable agreement with the experiment. This performance of QCE has made several authors interested in applying QCE to study the properties of liquids.

After applying QCE to water and ammonia, QCE has been applied to study the liquid properties of N-methylacetamide Ludwig *et al.* [4]. The authors have also applied the QCE in several other systems [5–8]. These systems have been studied using only the HF level of theory, which poorly describes quantum mechanical energies. Later, some authors applied the QCE to reinvestigate the same liquids with a relatively higher level of theory. Matisz *et al.* [9] used the QCE theory to investigate the properties of liquid methanol at the MP2/6-311++G(d,p) level of theory. Some authors have tested different levels of theory. Recently, Kuo and coworkers [10] have applied the QCE theory to determine some liquid properties of methanol after extensive exploration of the methanol clusters $(MeOH)_{n=2-14}$. The quantum chemical calculations have been performed at the four different levels of theory: B3LYP-CP/6-31+G(d,p), B3LYP-CP-D3/6-31+G(d,p), MP2/6-31+G(d,p), and MP2-CP/6-311++G(d,p). The authors calculated the clusters population, thermodynamics properties, and infrared spectrum at 300 K [10]. The QCE calculated infrared spectrum of liquid methanol agreed with experiment [10].

In addition to pure/neat liquids, the QCE theory has been used to study the properties of binary liquids. An extension of the QCE theory to study binary liquids (mixture of two different liquids) was proposed by the group of Kirchner in 2011 [11]. The proposed modified implementation of QCE has been applied to study the mixture of water and dimethylsulfoxide (DMSO) [11]. Later, the binary quantum cluster equilibrium (bQCE) theory was applied to study several mixtures of two liquids. Matisz *et al.* [12] have studied the binary mixture of methanol and water using bQCE theory. The study of the mixture of water and N-methylformamide has been reported by von Domaros and coworkers [13]. The authors reported the population of clusters in liquids in addition to some thermodynamic properties of the mixture. The mixing Gibbs free energy and the mixing enthalpy have been evaluated as a function of the mole fraction of N-methylformamide [13]. Ingenmey *et al.* [14] studied three binary mixtures: acetonitrile-acetone, benzene-acetone, and water-acetone. The study has been performed to predict the miscibility of the aforementioned binary systems. For each system, the population of clusters in liquid and the mixing Gibbs free energy have been provided [14]. Recently, Kutsyk *et al.* [15] have investigated the mixture of methanol and chloroform using the bQCE. The quantum mechanical calculations have been performed at the B3LYP/cc-pVTZ level of theory. They have evaluated the mixing enthalpy, concentration

* *E-mail: MalloumA@ufs.ac.za; Tel: +237 695 15 10 56*

profiles, and the liquid mixture's Raman and FTIR spectrum.

Moreover, QCE has been extended to study the activity coefficients in binary mixtures [16]. The proposed approach has been applied to the benzene–acetonitrile mixture [16]. Further investigations on binary mixtures have been performed by Marchelli and coworkers from the group of Kirchner [17,18]. Activity coefficients of a binary mixture of methanol and other alcohols (including ethanol, two propanols, and three butanols) have been calculated by Marchelli *et al.* using the bQCE theory [17]. The authors concluded that, in the mixture of methanol with alcohol, when the size of the alcohol is increased, they found a more significant deviation from an ideal mixture. However, when the branching of alcohols is increased, the authors found an ideal mixture [17]. Besides, a mixture of hexafluoroisopropanol and ethanol and hexafluoroisopropanol and methanol have been assessed using bQCE theory and classical molecular dynamics simulations [18]. The authors used up to six solvent molecules in pure and mixed solvents. Thermodynamic properties, including vaporization entropies and enthalpies, agree with experiment [18].

Besides pure and binary mixtures, QCE has been applied to study the conformer weighting in nicotine and their phosphorous derivatives and bulk systems [19,20]. Additionally, it is worth noting that Domaros and Perlt have investigated the effects of anharmonicity on the QCE results [21]. Domaros and Perlt [21] proposed a methodology to consider the anharmonicity effects, and they applied the methodology to the liquid hydrogen chloride. It has been found that the calculated properties are improved by including anharmonic effects [21]. Perlt *et al.* [22] have used the QCE theory to predict the ionic product of water using several quantum chemical levels of theory. Water clusters from monomer to decamer have been optimized using HF, and DFT functionals, including the D3 dispersion and counterpoise corrections, in addition to MP2 and DLPNO-CCSD(T) methods. For the specific case of the ionic product of water, the authors found that the results predicted at the B3LYP-D3/def2-TZVP have the tiniest mean absolute deviation from the experiment.

Examination of previous works shows that considerable investigations are reported in the literature using the QCE theory. Most of these works have been performed at a low level of theory. Moreover, very few works have extensively explored the sampling of cluster conformers. These limitations could affect the accuracy of the QCE predicted properties. Regarding the specific case of ethanol, Ludwig and coworkers [7,8] have applied the QCE to study liquid ethanol at the HF/6-31+G(d) level of theory. Only six conformers of ethanol clusters have been considered from monomer to hexamer. Thus, not all possible configurations of ethanol clusters have been located before applying the QCE. As seen in the results section, the accuracy of the QCE theory is dependent on the quantum chemical sampling of different conformers that could contribute to the liquid's population. Thus, it is essential to thoroughly sample different cluster configurations before applying the QCE for accurate predictions. Therefore, in this work, we applied the QCE theory to study the liquid properties of ethanol. We extensively explored cluster configurations using the MP2/aug-cc-pVDZ level of theory. The configurations have been initially generated using ABCluster [23,24]. Up to 484 different conformers of ethanol clusters, $(EtOH)_{n=2-6}$, have been selected at the MP2/aug-cc-pVDZ level of theory.

2 Methodology

This section briefly recalls the QCE theory in subsection 2.1. Then, we explain how the ethanol clusters have been generated and optimized quantum mechanically (see subsection 2.2).

2.1 Quantum cluster equilibrium (QCE) theory

The total partition function in the QCE theory can be written as follows:

$$Q^{tot}(N_p,V,T) = \prod_{p=1}^{N} \frac{1}{N_p!} \left[q_p^{rot}(T) q_p^{vib}(T) q_p^{el}(T) \left(\frac{2\pi m_p k_B T}{h^2} \right)^{3/2} \left(V - b_{xv} \sum_{p=1}^{N} N_p v_p \right) \exp\left\{ \frac{a_{mf} i(p)}{V k_B T} \right\} \right]^{N_p}. \quad (1)$$

where N_p is the number of isomers of size p. m_p is the mass of the isomer of size p. V is the volume. $\left(V - b_{xv}\sum_{p=1}^{N} N_p v_p\right)$ is the corrected volume of the system, where $v_p = i(p)v_1$ is the volume of an isomer of size p, which is equal to the product of the number of monomers, $i(p)$, times the volume of the monomer, v_1. $q_p^{rot}(T)$, $q_p^{vib}(T)$, and $q_p^{el}(T)$ is the rotational, vibrational, and electronic partition function of an isomer of size p, respectively.

$$q_p^{rot}(T) = \frac{\pi^{1/2}}{\sigma} \left(\frac{8\pi^2 k_B T}{h^2} \right)^{3/2} \sqrt{I_1 I_2 I_3} \quad (2)$$

I_1, I_2, I_3 are the principal moment of inertia. k_B, h are the Boltzmann and Planck constants, respectively, and T is the temperature. σ is the rotational symmetry number.

$$q_p^{vib}(T) = \prod_i \frac{1}{1 - \exp\left(-\frac{\Theta_{v,i}}{T} \right)} \quad (3)$$

$\Theta_{v,i}$ is the characteristic temperature.

$$q_p^{el}(T) = g_0 exp\left(-\frac{\varepsilon_0^{el}}{k_B T} \right). \quad (4)$$

ε_0^{el} and g_0 are the ground state electronic energy and its degeneracy, respectively. The electronic energies used in this work are zero-point energy (ZPE) corrected.

In this work, we applied the QCE theory to study the properties of liquid ethanol using the Peacemaker code of Kirchner and coworkers [25,26]. Peacemaker implements the QCE theory for pure and binary liquids. As input, Peacemaker needs the optimized Cartesian coordinates of all the conformers of the clusters to compute the moment of inertia of the rotational partition function. It also needs the binding energies and the vibrational frequencies to compute the electronic and the vibrational partition

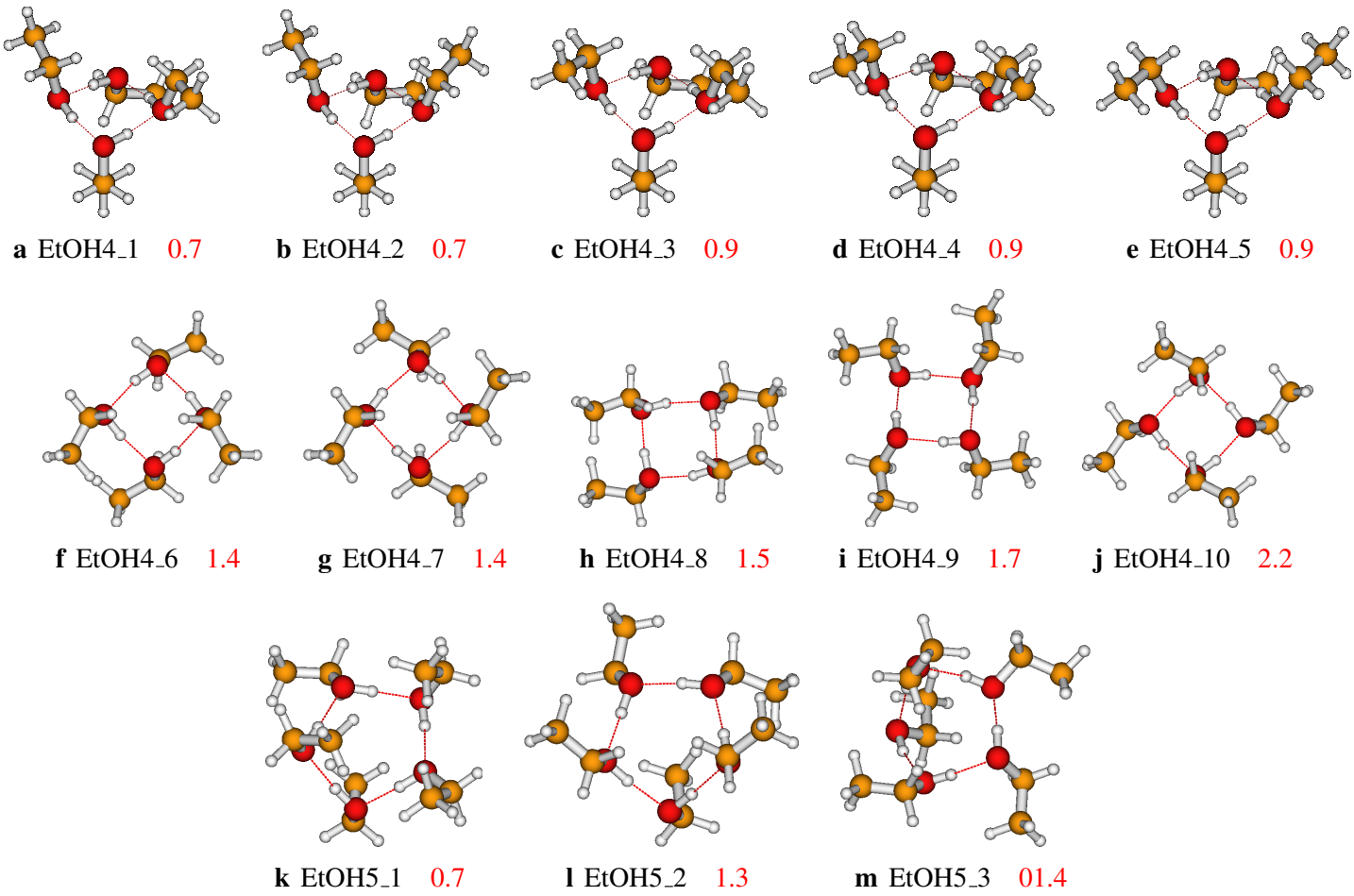

Fig. 1 Structures of the ethanol tetramer and pentamer that contribute to the population of liquid ethanol as will be discussed in subsection 3.1. The relative energies are calculated at the MP2/aug-cc-pVDZ level of theory (in kcal/mol).

functions. To determine a_{mf} and b_{xv}, Peacemaker needs an experimental property of the liquid that will serve as a reference to solve the polynomial equations. This experimental property can be the density of the liquid, the transition phase temperature, the isobar, or any combination of these properties. In this work, we used the density of liquid ethanol (0.7893 g/cm^3) and the transition temperature of ethanol from liquid to gas (351.52 K). The sampling of a_{mf} and b_{xv} has been performed between 0.0 and 2.0 and 0.5 and 1.5, respectively. Peacemaker's authors recommend these intervals. The sampling yielded the optimal values of 0.49 and 0.92 for a_{mf} and b_{xv}, respectively. These values confirm that the chosen intervals are correct. It should be noted that the Peacemaker code has been used successfully in several QCE theory applications to study pure and binary liquids [17,18,25].

2.2 Clusters' generation and quantum calculations

The accuracy of the QCE theory relies on the complete exploration of all possible conformers of the clusters that could contribute to the liquid population. Thus, an essential task for applying QCE starts by generating all possible clusters. In this work, the initial configurations of the clusters have been generated using the ABCluster code [23,24]. Details of the generation of the configurations are provided in our previous works [27–29]. The generated configurations are optimized at the MP2/aug-cc-pVDZ level of theory. The ABCluster code has been used in our previous works with reasonable accuracy to generate initial geometries [30–35].

3 Results and discussions

We start this section by presenting the clusters used in this work to perform the QCE predictions of liquid ethanol (see subsection 3.1). Then, the population of liquid ethanol is presented in subsection 3.2. The predicted thermodynamic properties are presented in subsection 3.3. Finally, the predicted population is used to determine the infrared spectrum of liquid ethanol (see subsection 3.4).

3.1 About the clusters

As mentioned above, the configurations generated by ABCluster have been fully optimized at the MP2/aug-cc-pVDZ level of the-

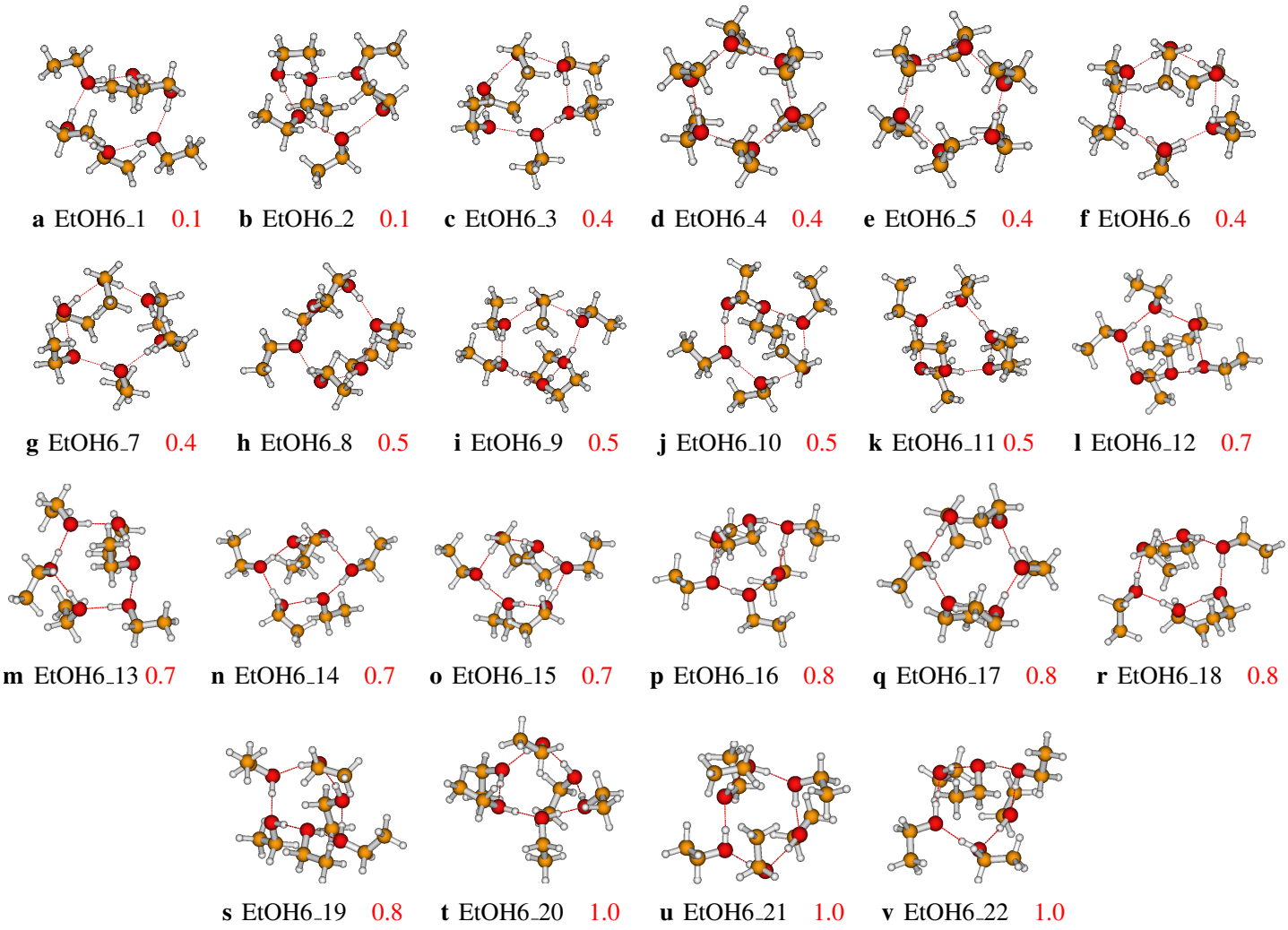

Fig. 2 Structures of the ethanol hexamer that contribute to the population of liquid ethanol as will be discussed in subsection 3.1. The relative energies are calculated at the MP2/aug-cc-pVDZ level of theory (in kcal/mol).

ory. Frequency calculation has also been performed at the same level of theory. Details of the generation can be found in our previous works on the ethanol clusters[27–29]. Up to 484 conformers of the ethanol clusters have been located at the MP2/aug-cc-pVDZ level of theory for clusters ranging from dimer ($n = 2$) to hexamer ($n = 6$). The located structures and their relative electronic energies have been published in our previous works[27–29]. It is worth recalling that the generation of clusters considered all the three monomers of ethanol (*trans*, *gauche*+, and *gauche*-). For each cluster size n, all possible combinations of the monomers have been considered to generate the configurations. These combinations lead to many located structures of the ethanol clusters from dimer to hexamer. Due to the mirror image between the *gauche*+ and *gauche*- conformers, we have concluded that each isomer of the ethanol clusters has a corresponding mirror image (enantiomer). This conclusion has been explicitly elaborated for the case of the ethanol dimer[29]. In this work, all mirror images have been discarded. That is to say; the 484 isomers have been obtained after excluding the mirror image of the isomers. In Figure 1 and Figure 2, EtOHx_y indicates the $y-$th isomer of the ethanol $x-$mer. We recommend the reader to read the previously published works for further details on the structures of the ethanol clusters used in this work[27–29].

We provided in the supporting information the Cartesian coordinates of the 484 structures considered in this work to apply the QCE on liquid ethanol. However, the structures that contribute to the population of liquid ethanol are reported in Figure 1 and Figure 2. Only structures that contribute with more than 1% to the population are considered in these figures. The contribution of configurations with 1% or lower are considered to be negligible. The structures are reported along with their relative energies (in kcal/mol) as calculated at the MP2/aug-cc-pVDZ level of theory. It is important to note that the relative energies consider all possible structures for the considered cluster size. Therefore, as can be seen in Figure 1 and Figure 2, the first isomer that contributes to the population is not necessarily the most stable one with relative

energy equals to 0.0 kcal/mol.

3.2 Predicted population of liquid ethanol

The predicted QCE population of liquid ethanol is reported in Figure 3. It should be noted that subsection 3.2 presents the population by cluster size and does not explicitly show the contribution of different configurations. This presentation is adopted to avoid cumbersomeness. Thus, for each cluster size n, we sum over the contribution of different isomers to determine the population as reported in Figure 3. The contribution of individual configurations to the population is provided in an Excel sheet as supporting information. The result indicates that the ethanol hexamer dominates the liquid ethanol population up to 320 K. Above 320 K, the ethanol pentamer dominates the population. The overall results show that the population of liquid ethanol comprises the contribution from tetramer, pentamer, and hexamer. The contribution of the ethanol monomer, dimer, and trimer to the population of liquid ethanol is negligible. Above 351 K (the transition temperature), the population is dominated exclusively by the ethanol monomer. In this range of temperatures, all the bondings linking the monomers together in a cluster are broken; therefore, only the ethanol monomer is found.

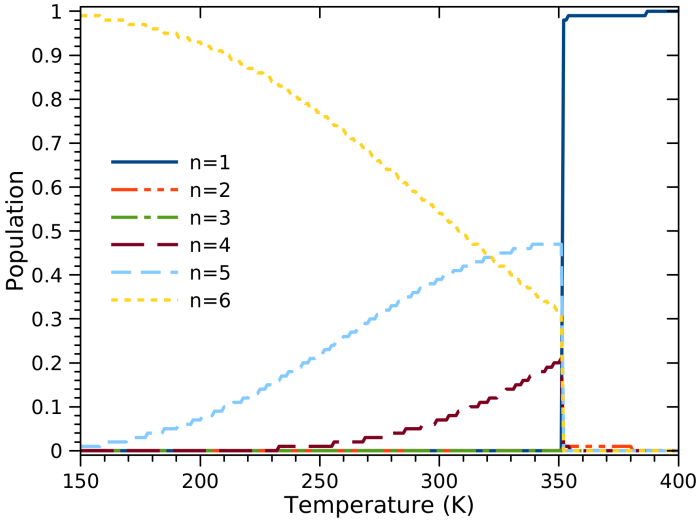

Fig. 3 QCE predicted population of liquid ethanol as a function of temperature from 150 to 400 K. For each cluster size n, the reported population is the sum of the population of different configurations of the considered cluster.

Previously, Ludwig *et al.*[7] applied the QCE theory to predict some thermodynamic properties of liquid ethanol. They performed their calculations at the HF/6-31G(d) level of theory. The calculations have been performed using clusters from monomer to hexamer, and only one configuration is used for each cluster size. Ludwig *et al.*[7] found that the population of the liquid ethanol between 250 and 350 K is constituted from the ethanol monomer, tetramer, and pentamer. They found that the ethanol dimer, trimer, and hexamer do not contribute to the population of the liquid ethanol. The difference between our prediction and the prediction of Ludwig *et al.*[7] can be ascribed to two facts: (1) we have used MP2/aug-cc-pVDZ level of theory, while they used HF/6-31G(d) level of theory, (2) and we have used 484 different configurations, while they used only six configurations. Considering the number of configurations we have used and the increased level of theory, our predicted population of liquid ethanol could be more reliable. It is worth recalling that, despite these differences, we predicted that the ethanol dimer and trimer do not contribute to the population of the liquid ethanol in agreement with the prediction of Ludwig *et al.*[7]. It is worth noting that other studies of liquid ethanol based on QCE at HF/6-31G(d) level of theory have been reported by Huelsekopf and Ludwig[36]. Borowski *et al.*[37] applied the QCE theory to study the liquid water, methanol, and ethanol after geometry optimizations at the B3LYP/6-311G(d,p) level of theory. They considered the ethanol clusters, $(EtOH)_n$, for $n = 1-6,\ 8$. Borowski *et al.*[37] found that only the ethanol monomer and pentamer contribute to the population of the liquid ethanol between 200 and 351 K. Unfortunately, similar to previous studies, only one configuration has been considered for each given cluster size[37]. Matisz *et al.*[38] have applied the QCE to the study of the liquid phase of some primary alcohols (methanol, ethanol, propan-1-ol, and butan-1-ol). For each alcohol, clusters from monomer to heptamer have been considered for QCE predictions. The authors stated that only cyclic configurations containing $g+tt$ or $g-tt$ ($t = trans$, $g+ = gauche+$, and $g- = gauche-$) had been selected based on previous studies at the B3LYP/6-31+G(d,p) level of theory[38]. Their predictions show that the population of liquid ethanol is dominated by ethanol heptamer, with a small contribution from hexamer and pentamer. They found a negligible contribution for dimer, trimer, and pentamer. As mentioned earlier, the fact that all possible configurations have not been used would be the main reason for the difference between our predicted population and that of Matisz and coworkers[38]. Recently, Teh, Hsu, and Kuo[10] have applied the QCE theory to study liquid methanol. They used methanol clusters from dimer to 14-mer at the B3LYP/6-31+G(d,p) level of theory. Their investigations show that an isomer of the methanol octamer dominates the population of liquid methanol[10].

Exploring the literature shows that only a few configurations of the ethanol clusters have been considered by previous authors in applying the QCE to liquid ethanol. This is understandable, considering the complexity of the PESs of the ethanol clusters. To properly apply the QCE to liquid ethanol and to expect accurate predictions, one had to locate all possible configurations of the ethanol clusters as large as possible. This exploration of all possible configurations has only been done in the present work, at an acceptable computational level of theory (the MP2/aug-cc-pVDZ level of theory), for ethanol clusters up to the ethanol hexamer. The fact that up to 484 configurations of the ethanol clusters have been used justifies the difference between our predictions and those of previous authors presented above. Based on this exploration, we can state that our predicted population of the liquid ethanol could be considered reliable. A warning regarding the current predicted population would be that the cluster size is limited to the hexamer. As stated above, Teh, Hsu, and Kuo[10] have found that a structure of the methanol octamer con-

tributes to the population of the liquid methanol. Although it is customary to assume that only small clusters would contribute to the population, it is unclear how small the cluster should be. Therefore, it is possible that the ethanol clusters larger than the ethanol hexamer, not considered here, may contribute to the population of liquid ethanol. However, considering the complexity of the PESs of the ethanol clusters (as outlined in our previous works[27–29]), it has not been possible for us to go beyond the hexamer at the MP2/aug-cc-pVDZ level of theory. To overcome this limitation, investigation of ethanol clusters larger than the hexamer at a cheaper, yet accurate, level of theory is advised for future works. The DFT functional PW6B95D3 has been benchmarked in our previous work[29] to be an accurate functional to reproduce the DLPNO-CCSD(T)/CBS level of theory. This DFT functional can be used for these investigations. Using QCE to predict the ionic product of water, Perlt *et al.*[22] have shown that a cheap computational level of theory can yield accurate predictions.

As mentioned above, only the sum of the contributions of all isomers of a given cluster to the population of the liquid ethanol is reported in subsection 3.2. To gain insights into the individual contributions of each isomer, we examined the case of the ethanol hexamer. The individual contributions of the isomers of the ethanol hexamer are reported in Figure 4. To avoid the cumbersomeness of Figure 4, only isomers that contribute with more than 2% are represented. The complete list of the isomers with their contribution as a function of temperature is provided in the supporting information. It can be seen in Figure 4 that several isomers of the ethanol hexamer have a considerable contribution to the population of the liquid ethanol. The first two isomers with the highest contributions are **EtOH6_22** and **EtOH6_18**, lying 1.0 kcal/mol and 0.8 kcal/mol above the most stable. Interestingly, the most stable isomer (based on the electronic energy) does not contribute to the predicted population of the liquid ethanol. This result highlights the importance of thoroughly exploring the ethanol clusters to obtain a reliable population prediction. Although it is impossible to know which isomer can contribute in advance, our results show that the isomers that contribute have their relative electronic energies within ∼2.0 kcal/mol. Therefore, thoroughly exploring the clusters within a few kcal/mol would lead to accurate population prediction.

3.3 QCE predicted thermodynamic properties

After the prediction of the population of the liquid ethanol, some thermodynamic properties have been estimated for temperatures ranging from 150 to 400 K. The estimated thermodynamic properties include the heat capacity at constant pressure, C_p, the heat capacity at constant volume, C_v, the internal energy, U, the enthalpy, H, the entropy, S, and the Gibbs free energy, G. These QCE-predicted thermodynamic properties are reported in the supporting information. However, for some selected temperatures, we provided the experimental and the QCE predicted heat capacity at constant pressure in Table 1. As can be seen in Table 1, the QCE predicted heat capacity at constant pressure is closer to the experimental heat capacity of gas-phase ethanol than that of liquid-phase ethanol at room temperature (298.15 K). This discrepancy has been reported and discussed previously in the case of liquid water[25]. The discrepancy between the QCE-predicted heat capacity and the experimental one is ascribed to the limitation in calculating the total partition function. The vibrational partition function is calculated in the framework of harmonic approximation. Thus, anharmonic effects can considerably affect the predicted properties. In addition, only interactions between ethanol molecules inside clusters are treated correctly, while a mean-field approximation represents interactions between different clusters (mainly CH···O and OH···O interactions)[25]. Improvement of these limitations would yield more accurate QCE predictions.

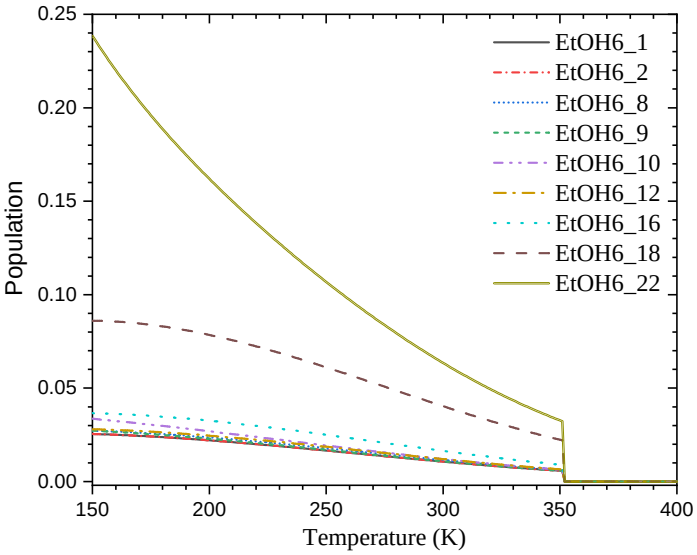

Fig. 4 Contributions of individual isomers of the ethanol hexamer to the population of the liquid ethanol, reported in Figure 3.

3.4 Predicted infrared spectrum of liquid ethanol

Using the predicted population of the liquid ethanol, we determine its infrared spectrum using Equation 5.

$$I(\omega,T)=\sum_i N_i(T)\sum_k \frac{I_{ik}}{\pi}\frac{\gamma_{ik}}{(\omega-\omega_{ik})^2+\gamma_{ik}^2}, \qquad (5)$$

where $N_i(T)$ is the probability of configuration i at temperature T. I_{ik} and ω_{ik} are the intensity and the central frequency of the k^{th} peak of configuration i. γ_{ik} is half of FWHM (full width at half maximum). In this work, γ_{ik} is considered to be constant, where $\gamma_{ik}=20.0\,\mathrm{cm}^{-1}$ for frequencies below $2000\,\mathrm{cm}^{-1}$ and $\gamma_{ik}=40.0\,\mathrm{cm}^{-1}$ for frequencies above $2000\,\mathrm{cm}^{-1}$. Frequencies above $2000\,\mathrm{cm}^{-1}$ correspond to OH and CH stretching, while frequencies below $2000\,\mathrm{cm}^{-1}$ correspond to bending, wagging and twisting of the molecular coordinates. In order to account for anharmonic effects on the calculated frequencies, we applied a scale factor of 0.959 to all frequencies. The calculated infrared

Table 1 Heat capacity at different temperatures predicted with QCE. C_p(gas) and C_p(liquid) are retrieved from the NIST Chemistry WebBook[39,40]. 1 atm is the pressure considered for all temperatures.

T(K)	C_p(gas)	C_p(liquid)[41]	C_p(QCE)
300.00		112.75	70.52
305.00		115.43	71.33
310.00		118.12	72.14
315.00		120.80	72.79
320.00		123.49	73.76
325.00		126.17	74.58
330.00		128.85	75.40
340.00		134.22	77.03
350.00		139.59	78.67
356.55	75.70		75.46
360.00	74.57		75.62
361.75	76.40		75.77
367.90	75.52		76.38
370.01	76.00		76.62
371.85	77.70		76.88
380.00	77.46		77.99
387.25	79.80		79.02
388.85	80.00		79.32
400.08	80.40		80.99

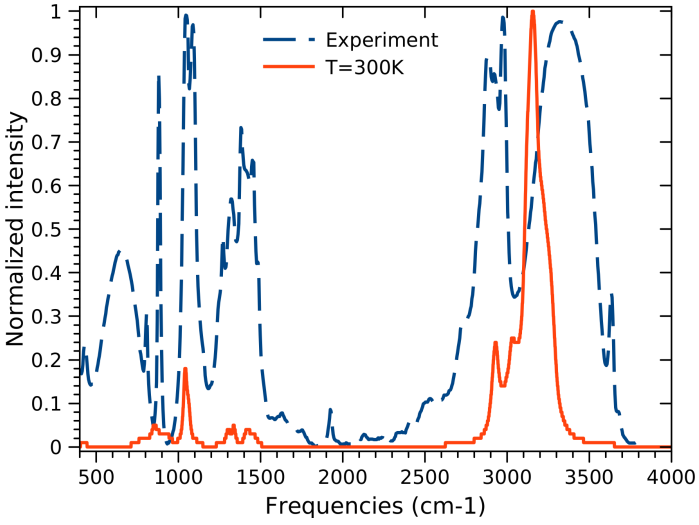

Fig. 5 Predicted IR spectrum of liquid ethanol for temperature $T = 300\,\mathrm{K}$. The spectrum is generated using the Equation 5.

spectrum of the liquid ethanol at $T = 300\,\mathrm{K}$ is reported in Figure 5. In addition, we have also reported in Figure 5 the experimental infrared spectrum of liquid ethanol[42]. Both the calculated and the experimental spectra are normalized to unity for the region 500 to 4000 cm^{-1}. We have calculated the infrared spectra for different temperatures $T \in [150, 200, 250, 300, 350, 400]\mathrm{K}$ and reported the curves in the supporting information. We noted that the calculated spectrum for temperatures in the liquid phase $T \in [150, 200, 250, 300, 350]\mathrm{K}$ are found to be almost identical. However, for $T = 400\,\mathrm{K}$, where the population is dominated exclusively by the ethanol monomer, the calculated IR spectrum is equal to that of the ethanol monomer.

It can be seen in Figure 5 that the calculated infrared spectrum of the liquid ethanol is in qualitative agreement with the experiment. Despite the qualitative agreement, we noted that the intensity of the predicted peaks is lower than those of the experimental peaks in the frequency region lower than 2000 cm^{-1}. The discrepancy between the calculated and the experimental infrared spectrum is ascribable to anharmonic effects (Fermi resonances): overtones and combination bands. These effects have been highlighted in protonated methanol clusters[43] and methyl and methoxy groups[44]. Teh, Hsu, and Kuo[10] applied the QCE theory to calculate the infrared spectrum of the liquid methanol at $T = 300\,\mathrm{K}$. The authors have used four different levels of theory. It came out that the infrared spectra predicted at these levels of theory display similar features.

4 Conclusions

In this work, we applied the quantum cluster equilibrium theory (QCE) to study the properties of liquid ethanol. We started by exploring the PESs of the ethanol clusters from dimer to hexamer using classical molecular dynamics as implemented in the ABCluster code. The generated geometries have been optimized at the MP2/aug-cc-pVDZ level of theory. We located up to 484 different configurations of the ethanol clusters at the MP2/aug-cc-pVDZ level of theory. The interaction energies, vibrational frequencies, and Cartesian coordinates of the structures have been used to determine the total QCE partition function and predict the liquid ethanol's properties. The result shows that the ethanol hexamer dominates the predicted population of liquid ethanol. It has been found that the ethanol pentamer and the ethanol tetramer contribute to the population of liquid ethanol along with the ethanol hexamer. The prediction indicated that the ethanol monomer, dimer, and trimer do not contribute to the population of liquid ethanol. Besides, the infrared spectrum of the liquid ethanol has been calculated based on the QCE predicted population. The calculated infrared spectrum is in qualitative agreement with the experiment. The predicted intensities of some peaks are smaller than the experiment peaks. The difference is attributed to the anharmonic effects. Moreover, thermodynamic properties such as the heat capacity at constant pressure, the heat capacity at constant volume, the internal energy, the enthalpy, the entropy, and the Gibbs free energy of the liquid ethanol are predicted and reported using the QCE.

Despite the efforts made in this work toward achieving accuracy and reliability, some issues still need to be considered, which could affect the accuracy of the predictions made in this work. These issues include:

Cluster size. As mentioned in the previous section, the fact that the ethanol clusters larger than the hexamer have not been considered in this work may affect the current QCE predictions. Therefore, a more accurate work should include larger-sized clusters, which has not been possible at the MP2/aug-cc-pVDZ level of theory, considering the expense

of the level of theory. PW6B95D3 is recommended for future works on larger-sized ethanol clusters based on our previous works.

Basis set superposition error (BSSE). The total partition function depends on the accuracy of the interaction energy of the clusters, which in turn is considerably affected by BSSE. These corrections have not been considered in this work, which could also affect the reliability of the QCE predictions reported in this work. Thus, including BSSE corrections, through CBS (complete basis set) extrapolations or counterpoise corrections, could increase the reliability of the study. Nevertheless, it should be noted that including counterpoise corrections with a relatively large basis set (TZ or higher) could worsen the predictions [22].

Anharmonicity. The total partition function depends on the vibrational frequencies. In this work, the vibrational frequencies are calculated in the framework of the rigid rotor and harmonic approximations. Therefore, anharmonic effects could considerably affect the total partition function, especially in hydrogen-bonded molecular systems. Thus, anharmonic corrections should be considered in future works for accurate predictions.

Acknowledgements

A.M. is grateful to The Abdus Salam International Centre for Theoretical Physics (ICTP) for funding his visit to Tunisia, where the work has been performed. This work has received support from the South African National Research Foundation (NRF, Grant number 145414). We would also like to thank the Central Research Fund of the University of the Free State. The authors are grateful to the Center for High Performance Computing (CHPC, Grant number CHEM0947) in South Africa for computational resources.

Disclosure statement

There are no conflicts of interest to declare.

Data availability statement

The data used in this work is provided in the manuscript or in the supporting information.

Supporting information

The supporting information includes:

- The Cartesian coordinates of the 484 configurations of the ethanol clusters
- The QCE predicted population of the liquid ethanol
- Data of the predicted thermodynamic properties
- The calculated infrared spectra of the liquid ethanol at different temperatures.

References

1 Weinhold, F. Quantum cluster equilibrium theory of liquids: General theory and computer implementation. *J. Chem. Phys.* **1998**, *109*, 367–372.

2 Ludwig, R.; Weinhold, F.; Farrar, T. Quantum cluster equilibrium theory of liquids part I: Molecular clusters and thermodynamics of liquid ammonia. *Ber. Bunsen. Phys. Chem.* **1998**, *102*, 197–204.

3 Ludwig, R.; Weinhold, F.; Farrar, T. Quantum cluster equilibrium theory of liquids part II: Temperature dependent chemical shifts, quadrupole coupling constants and vibrational frequencies in liquid ammonia. *Ber. Bunsen. Phys. Chem.* **1998**, *102*, 205–212.

4 Ludwig, R.; Reis, O.; Winter, R.; Weinhold, F.; Farrar, T. Quantum cluster equilibrium theory of liquids: temperature dependence of hydrogen bonding in liquid N-methylacetamide studied by IR spectra. *J. Phys. Chem. B* **1998**, *102*, 9312–9318.

5 Ludwig, R.; Weinhold, F.; Farrar, T. Theoretical study of hydrogen bonding in liquid and gaseous N-methylformamide. *J. Chem. Phys.* **1997**, *107*, 499–507.

6 Ludwig, R.; Weinhold, F.; Farrar, T. Structure of liquid N-methylacetamide: temperature dependence of NMR chemical shifts and quadrupole coupling constants. *J. Phys. Chem. A* **1997**, *101*, 8861–8870.

7 Ludwig, R.; Weinhold, F.; Farrar, T. Quantum cluster equilibrium theory of liquids: molecular clusters and thermodynamics of liquid ethanol. *Mol. Phys.* **1999**, *97*, 465–477.

8 Ludwig, R.; Weinhold, F.; Farrar, T. Quantum cluster equilibrium theory of liquids: temperature dependent chemical shifts, quadrupole coupling constants and vibrational frequencies in liquid ethanol. *Mol. Phys.* **1999**, *97*, 479–486.

9 Matisz, G.; Fabian, W. M.; Kelterer, A.-M.; Kunsági-Máté, S. Weinhold's QCE model–A modified parameter fit. Model study of liquid methanol based on MP2 cluster geometries. *J. Mol. Struct.* **2010**, *956*, 103–109.

10 Teh, S.; Hsu, P.-J.; Kuo, J.-L. Size of the hydrogen bond network in liquid methanol: a quantum cluster equilibrium model with extensive structure search. *Phys. Chem. Chem. Phys.* **2021**, *23*, 9166–9175.

11 Brüssel, M.; Perlt, E.; Lehmann, S. B.; von Domaros, M.; Kirchner, B. Binary systems from quantum cluster equilibrium theory. *J. Chem. Phys.* **2011**, *135*, 194113.

12 Matisz, G.; Kelterer, A.-M.; Fabian, W.; Kunsági-Máté, S. Structural properties of methanol–water binary mixtures within the quantum cluster equilibrium model. *Phys. Chem. Chem. Phys.* **2015**, *17*, 8467–8479.

13 von Domaros, M.; Jähnigen, S.; Friedrich, J.; Kirchner, B. Quantum cluster equilibrium model of N-methylformamide–water binary mixtures. *J. Chem. Phys.* **2016**, *144*, 064305.

14 Ingenmey, J.; von Domaros, M.; Kirchner, B. Predicting miscibility of binary liquids from small cluster QCE calculations. *J. Chem. Phys.* **2017**, *146*, 154502.

15 Kutsyk, A.; Ilchenko, O.; Pilhun, Y.; Nikonova, V.; Obukhovsky, V. Complex formation in methanol-chloroform solutions: Vibrational spectroscopy and quantum cluster equilibrium study. *J. Mol. Liq.* **2022**, *367*, 120499.

16 Ingenmey, J.; Blasius, J.; Marchelli, G.; Riegel, A.; Kirchner, B. A

cluster approach for activity coefficients: General theory and implementation. *J. Chem. Eng. Data* **2019**, *64*, 255–261.

17 Marchelli, G.; Ingenmey, J.; Kirchner, B. Activity coefficients of binary methanol alcohol mixtures from cluster weighting. *ChemistryOpen* **2020**, *9*, 774–785.

18 Marchelli, G.; Ingenmey, J.; Hollóczki, O.; Chaumont, A.; Kirchner, B. Hydrogen Bonding and Vaporization Thermodynamics in Hexafluoroisopropanol-Acetone and-Methanol Mixtures. A Joined Cluster Analysis and Molecular Dynamic Study. *ChemPhysChem* **2022**, *23*, e202100620.

19 Blasius, J.; Kirchner, B. Cluster-weighting in bulk phase vibrational circular dichroism. *J. Phys. Chem. B* **2020**, *124*, 7272–7283.

20 Taherivardanjani, S.; Blasius, J.; Brehm, M.; Dotzer, R.; Kirchner, B. Conformer Weighting and Differently Sized Cluster Weighting for Nicotine and Its Phosphorus Derivatives. *J. Phys. Chem. A* **2022**, *126*, 7070–7083.

21 von Domaros, M.; Perlt, E. Anharmonic effects in the quantum cluster equilibrium method. *J. Chem. Phys.* **2017**, *146*, 124114.

22 Perlt, E.; von Domaros, M.; Kirchner, B.; Ludwig, R.; Weinhold, F. Predicting the ionic product of water. *Sci. Rep.* **2017**, *7*, 10244.

23 Zhang, J.; Dolg, M. ABCluster: the artificial bee colony algorithm for cluster global optimization. *Phys. Chem. Chem. Phys.* **2015**, *17*, 24173–24181.

24 Zhang, J.; Dolg, M. Global optimization of clusters of rigid molecules using the artificial bee colony algorithm. *Phys. Chem. Chem. Phys.* **2016**, *18*, 3003–3010.

25 Kirchner, B.; Spickermann, C.; Lehmann, S. B.; Perlt, E.; Langner, J.; von Domaros, M.; Reuther, P.; Uhlig, F.; Kohagen, M.; Brüssel, M. What can clusters tell us about the bulk?: Peacemaker: Extended quantum cluster equilibrium calculations. *Comput. Phys. Commun.* **2011**, *182*, 1428–1446.

26 von Domaros, M.; Perlt, E.; Ingenmey, J.; Marchelli, G.; Kirchner, B. Peacemaker 2: Making clusters talk about binary mixtures and neat liquids. *SoftwareX* **2018**, *7*, 356–359.

27 Malloum, A.; Fifen, J. J.; Conradie, J. Exploration of the potential energy surface of the ethanol hexamer. *J. Chem. Phys.* **2019**, *150*, 124308.

28 Malloum, A.; Fifen, J. J.; Conradie, J. Theoretical infrared spectrum of the ethanol hexamer. *Int. J. Quantum Chem.* **2020**, *120*, e26234.

29 Malloum, A.; Fifen, J. J.; Conradie, J. Exploration of the Potential Energy Surfaces of Small Ethanol Clusters. *Phys. Chem. Chem. Phys.* **2020**, *22*, 13201–13213.

30 Malloum, A.; Conradie, J. Potential energy surface of the thiophene pentamer and non-covalent interactions. *Int. J. Quantum Chem.* **2022**, *122*, e26840.

31 Malloum, A.; Conradie, J. Structures, binding energies and non-covalent interactions of furan clusters. *J. Mol. Graph. Mod.* **2022**, *111*, 108102.

32 Malloum, A.; Conradie, J. Non-covalent interactions in small thiophene clusters. *J. Mol. Liq.* **2022**, *347*, 118301.

33 Malloum, A.; Conradie, J. Non-Covalent Interactions in Dimethylsulfoxide (DMSO) Clusters and DFT Benchmarking. *J. Mol. Liq.* **2022**, *350*, 118522.

34 Malloum, A.; Conradie, J. Molecular simulations of the adsorption of aniline from waste-water. *J. Mol. Graph. Mod.* **2022**, *117*, 108287.

35 Malloum, A.; Conradie, J. Dimethylformamide clusters: non-covalent bondings, structures and temperature-dependence. *Mol. Phys.* **2022**, *120*, e2118188.

36 Huelsekopf, M.; Ludwig, R. Temperature dependence of hydrogen bonding in alcohols. *J. Mol. Liq.* **2000**, *85*, 105–125.

37 Borowski, P.; Jaroniec, J.; Janowski, T.; Woliński, K. Quantum cluster equilibrium theory treatment of hydrogen-bonded liquids: Water, methanol and ethanol. *Mol. Phys.* **2003**, *101*, 1413–1421.

38 Matisz, G.; Kelterer, A.-M.; Fabian, W. M.; Kunsagi-Mate, S. Application of the quantum cluster equilibrium (QCE) model for the liquid phase of primary alcohols using B3LYP and B3LYP-D DFT methods. *J. Phys. Chem. B* **2011**, *115*, 3936–3941.

39 Stromsoe, E. Heat capacity of alcohol vapors at atmospheric pressure. *J. Chem. Eng. Data* **1970**, *15*, 286–290.

40 Lemmon, E. W.; Bell, I. H.; Huber, M. L.; McLinden, M. O. *NIST Chemistry WebBook, NIST Standard Reference Database Number 69*; Eds. P.J. Linstrom and W.G. Mallard: National Institute of Standards and Technology, Gaithersburg MD, 20899, 2023.

41 Pedersen, M. J.; Kay, W. B.; Hershey, H. C. Excess enthalpies, heat capacities, and excess heat capacities as a function of temperature in liquid mixtures of ethanol+ toluene, ethanol+ hexamethyldisiloxane, and hexamethyldisiloxane+ toluene. *J. Chem. Thermodynam.* **1975**, *7*, 1107–1118.

42 Wallace, W. E. *NIST Chemistry WebBook, NIST Standard Reference Database Number 69*; Eds. P.J. Linstrom and W.G. Mallard: National Institute of Standards and Technology, Gaithersburg MD, 20899, 2023.

43 Lin, C.-K.; Huang, Q.-R.; Li, Y.-C.; Nguyen, H.-Q.; Kuo, J.-L.; Fujii, A. Anharmonic coupling revealed by the vibrational spectra of solvated protonated methanol: Fermi resonance, combination bands, and isotope effect. *J. Phys. Chem. A* **2021**, *125*, 1910–1918.

44 Sibert III, E. L.; Tabor, D. P.; Kidwell, N. M.; Dean, J. C.; Zwier, T. S. Fermi resonance effects in the vibrational spectroscopy of methyl and methoxy groups. *J. Phys. Chem. A* **2014**, *118*, 11272–11281.